

Volume 35, Issue 4

April 2025

JOURNAL OF FLUORESCENCE

ISSN

1053-0509

EISSN

1573-4994

JCR ABBREVIATION

J FLUORESC

ISO ABBREVIATION

J. Fluoresc.

Journal information

EDITION

Science Citation Index Expanded (SCIE)

CATEGORY

CHEMISTRY, ANALYTICAL

CHEMISTRY, PHYSICAL

BIOCHEMICAL RESEARCH METHODS

LANGUAGES

English

REGION

USA

1ST ELECTRONIC JCR YEAR

2000

Publisher information

PUBLISHER

SPRINGER/PLENUM PUBLISHERS

ADDRESS

233 SPRING ST, NEW YORK, NY 10013

PUBLICATION FREQUENCY

6 issues/year

Journal's performance

Journal Impact Factor

The Journal Impact Factor (JIF) is a journal-level metric calculated from data indexed in the Web of Science Core Collection. It should be used with careful attention to the many factors that influence citation rates, such as the volume of publication and citations characteristics of the subject area and type of journal. The Journal Impact Factor can complement expert opinion and informed peer review. In the case of academic evaluation for tenure, it is inappropriate to use a journal-level metric as a proxy measure for individual researchers, institutions, or articles. Learn more

2024 JOURNAL IMPACT FACTOR

3.1

View calculation

JOURNAL IMPACT FACTOR WITHOUT SELF CITATIONS

2.8

View calculation

Journal Impact Factor Trend 2024

Export

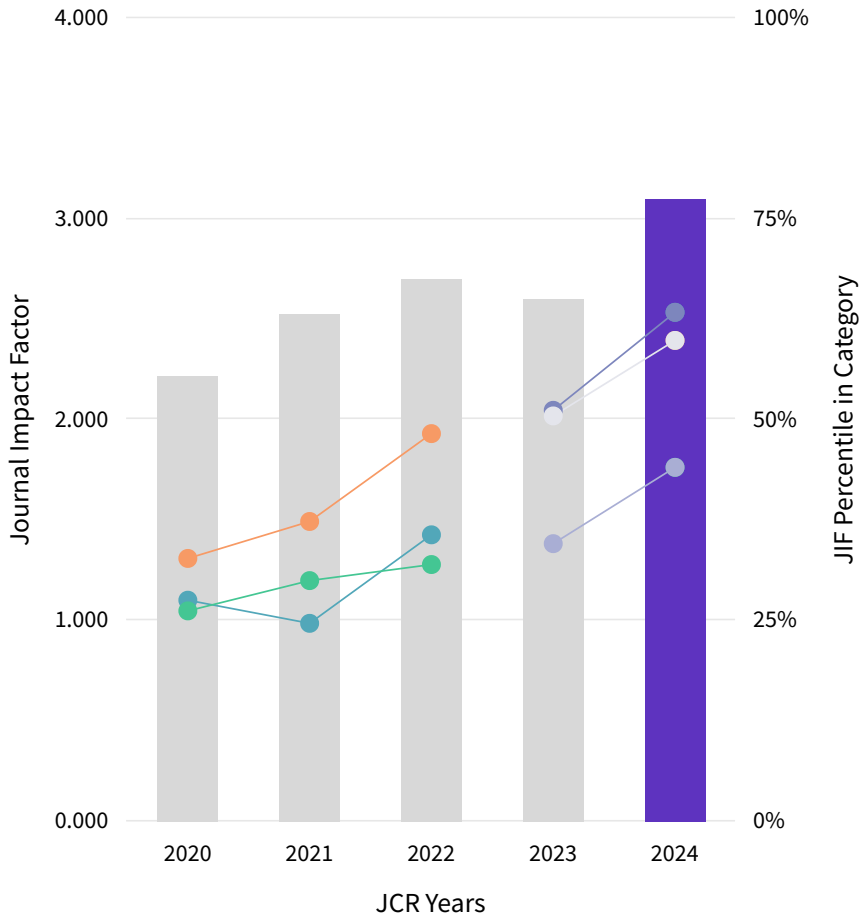
Journal Impact Factor contributing items

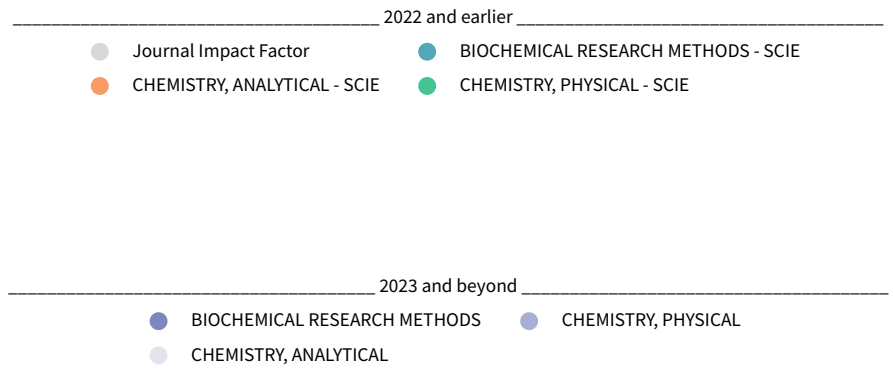
Export

Citable items (671) Citing Sources (499)

TITLE	CITATION COUNT
Molecular Dynamics and Multi-Spectroscopic of the Interaction Behavi…	74
A Review on Schiff Base as a Versatile Fluorescent Chemo-sensors Tool for…	31

15





View all years

Microwave-Assisted Green Synthesis of Carbon Quantum Dots Derived from…	27
Synthesis, Optoelectronic and Photoluminescent Characterizations of…	25
A Review on Characterization Techniques for Carbon Quantum Dots and Their…	23
Schiff Bases: A Versatile Fluorescence Probe in Sensing Cations	19
Hydrazone-based Materials; DFT, TD-DFT, NBO Analysis, Fukui Function, MESP…	18
Recent Applications of Quantum Dots in Pharmaceutical Analysis	18
A Review on Metal Ion Sensors Derived from Chalcone Precursor	16
The Green Synthesis of Carbon Quantum Dots through One-step Hydrothermal…	16

View All in Web of Science

Journal Citation Indicator (JCI)

Export

0.64

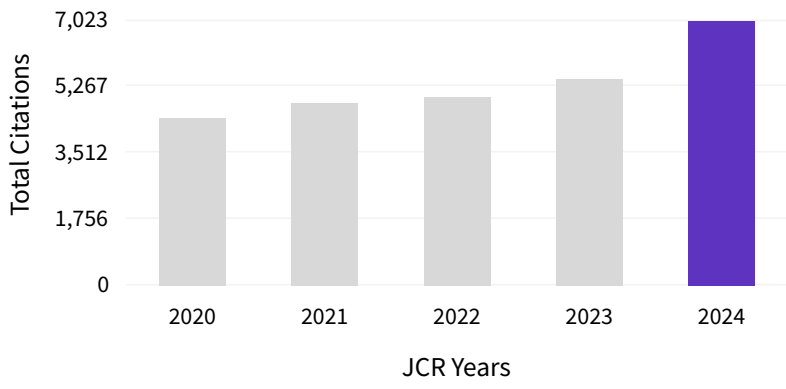
The Journal Citation Indicator (JCI) is the average Category Normalized Citation Impact (CNCI) of citable items (articles & reviews) published by a journal over a recent three year period. The average JCI in a category is 1. Journals with a JCI of 1.5 have 50% more citation impact than the average in that category. It may be used alongside other metrics to help you evaluate journals. Learn more

Total Citations

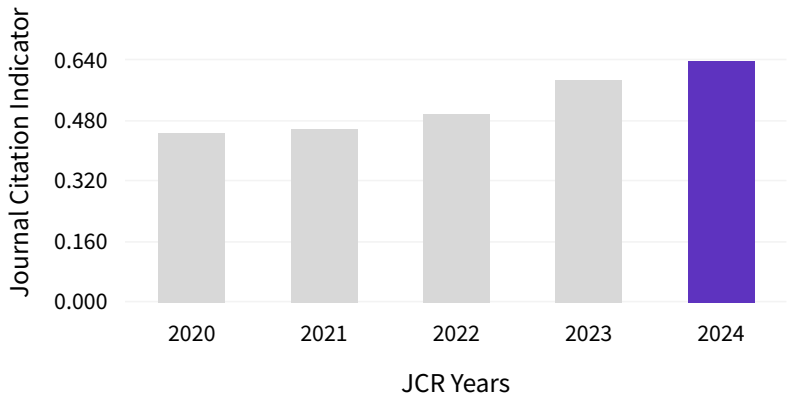
Export

7,023

The total number of times that a journal has been cited by all journals included in the database in the JCR year. Citations to journals listed in JCR are compiled annually from the JCR years combined database, regardless of which JCR edition lists the journal.



15



View all years

View all years

Citation distribution

Export

The Citation Distribution shows the frequency with which items published in the year or two years prior were cited in the JCR data year (i.e., the component of the calculation of the JIF). The graph has similar functionality as the JIF Trend graph, including hover-over data descriptions for each data point, and an interactive legend where each data element's legend can be used as a toggle. You can view Articles, Reviews, or Non-Citable (other) items to the JIF numerator. Learn more

ARTICLE CITATION MEDIAN

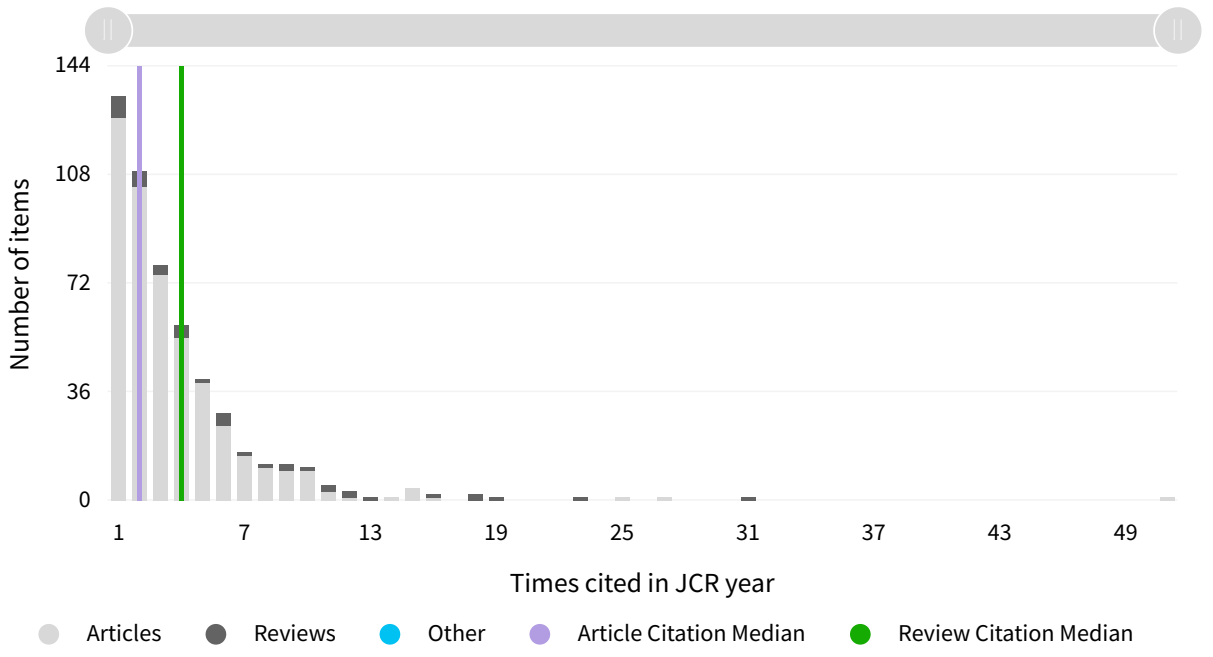
2

REVIEW CITATION MEDIAN

4

UNLINKED CITATIONS

49



TIMES CITED

0

ARTICLES

143

REVIEWS

4

OTHER

16

Open Access (OA)

Export

The data included in this tile summarizes the items published in the journal in the JCR data year and in the previous two years. This three-year set of published items is used to provide descriptive analysis of the content and community of the journal. Learn more

Items

TOTAL CITABLE	% OF CITABLE OA
1,186	6.91%

Citations*

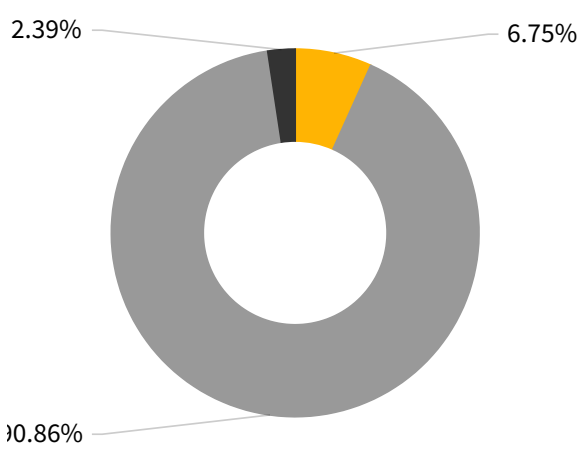
TOTAL CITABLE	% OF CITABLE OA
2,420	9.30%

15

CITABLE

GOLD OPEN ACCESS
82 / 6.75%

SUBSCRIPTION AND FREE TO READ
1,104 / 90.86%



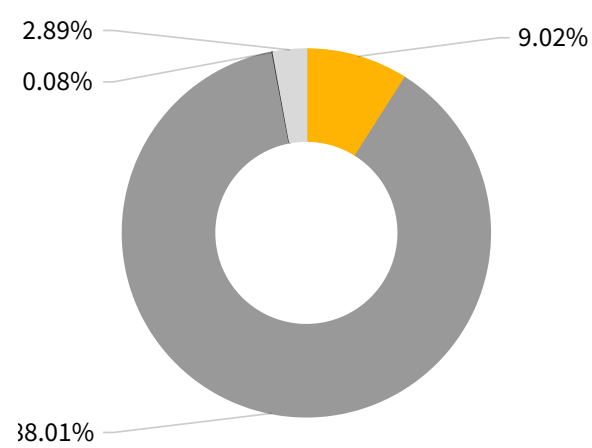
NON-CITABLE

OTHER (NON CITABLE ITEMS)
29 / 2.39%

CITABLE

GOLD OPEN ACCESS
225 / 9.02%

SUBSCRIPTION AND FREE TO READ
2,195 / 88.01%



NON-CITABLE

OTHER (NON CITABLE ITEMS)
2 / 0.08%

UNLINKED CITATIONS
72 / 2.89%

*Citations in 2024 to items published in [2022 - 2024]

Rank by Journal Impact Factor

Journals within a category are sorted in descending order by Journal Impact Factor (JIF) resulting in the Category Ranking below. A separate rank is shown for each category in which the journal is listed in JCR. Beginning in 2023, ranks are calculated by category.
Learn more

CATEGORY
BIOCHEMICAL RESEARCH METHODS

32/86

JCR YEAR	JIF RANK	JIF QUARTILE	JIF PERCENTILE
2024	32/86	Q2	63.4
2023	42/85	Q2	51.2

CATEGORY
CHEMISTRY, ANALYTICAL

45/111

JCR YEAR	JIF RANK	JIF QUARTILE	JIF PERCENTILE
2024	45/111	Q2	59.9
2023	53/106	Q2	50.5

Rank by JIF before 2023 for BIOCHEMICAL RESEARCH METHODS

EDITION
Science Citation Index Expanded (SCIE)

JCR YEAR	JIF RANK	JIF QUARTILE	JIF PERCENTILE
2022	50/77	Q3	35.7
2021	60/79	Q4	24.68
2020	57/78	Q3	27.56
2019	49/77	Q3	37.01

Rank by JIF before 2023 for CHEMISTRY, ANALYTICAL

EDITION
Science Citation Index Expanded (SCIE)

JCR YEAR	JIF RANK	JIF QUARTILE	JIF PERCENTILE
2022	45/86	Q3	48.3
2021	55/87	Q3	37.36
2020	59/87	Q3	32.76
2019	48/86	Q3	44.77

15

Rank by Journal Citation Indicator (JCI)

Journals within a category are sorted in descending order by Journal Citation Indicator (JCI) resulting in the Category Ranking below. A separate rank is shown for each category in which the journal is listed in JCR. Data for the most recent year is presented at the top of the list, with other years shown in reverse chronological order. Learn more

CATEGORY

BIOCHEMICAL RESEARCH METHODS

46/86

JCR YEAR	JCI RANK	JCI QUARTILE	JCI PERCENTILE
2024	46/86	Q3	47.09
2023	49/85	Q3	42.94
2022	61/83	Q3	27.11
2021	62/84	Q3	26.79
2020	63/82	Q4	23.78
2019	63/82	Q4	23.78
2018	67/82	Q4	18.90

CATEGORY

CHEMISTRY, ANALYTICAL

54/111

JCR YEAR	JCI RANK	JCI QUARTILE	JCI PERCENTILE
2024	54/111	Q2	51.80
2023	57/106	Q3	46.70
2022	63/99	Q3	36.87
2021	64/99	Q3	35.86
2020	62/98	Q3	37.24
2019	58/98	Q3	41.33
2018	60/97	Q3	38.66

Citation network

Cited Half-life

5.0 years

The Cited Half-Life is the median age of the items in this journal that were cited in the JCR year. Half of a journal's cited items were published more recently than the cited half-life.

TOTAL NUMBER OF CITES

7,023

NON SELF-CITATIONS

6,388

SELF-CITATIONS

635

Citing Half-life

6.3 years

The Citing Half-Life is the median age of items in other publications cited by this journal in the JCR year.

TOTAL NUMBER OF CITES

24,871

NON SELF-CITATIONS

24,236

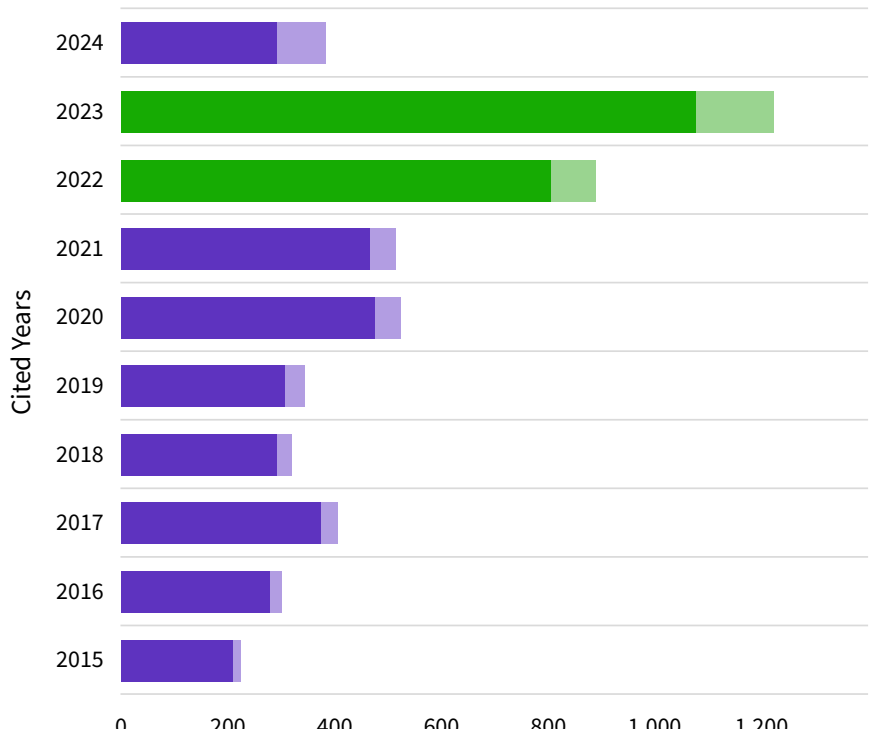
SELF-CITATIONS

635

Cited Half-life Data | Citing Half-life Data

Export

15

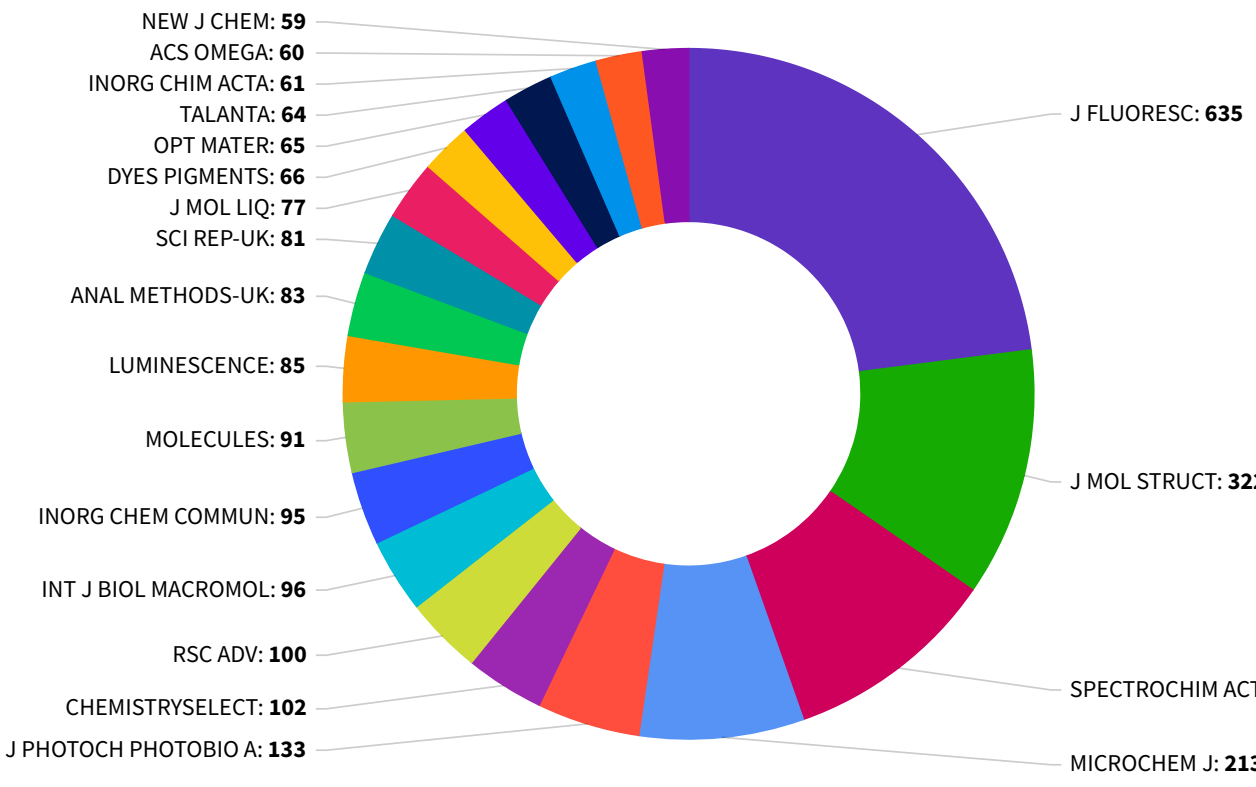


CITED YEAR	# OF CITES FROM 2024	CUMULATIVE %	# OF CITING SOURCES
All years	**7,023 citations**	**100.00%**	**1,073 sources**
2024	382 citations	5.44%	138 sources
2023	1,223 citations	22.85%	374 sources
2022	889 citations	35.51%	300 sources
2021	513 citations	42.82%	224 sources
2020	523 citations	50.26%	245 sources
2019	343 citations	55.15%	178 sources
2018	320 citations	59.70%	180 sources
2017	406 citations	65.48%	193 sources
2016	301 citations	69.77%	169 sources
2015	224 citations	72.96%	129 sources

Journal Citation Relationships

Cited Data Citing Data

Top 20 journals citing J FLUORESC by number of citations



Content metrics

Source data

15

Average JIF Percentile

Export

This tile shows the breakdown of document types published by the journal. Citable Items are Articles and Reviews. For the purposes of calculating JIF, a JCR year considers the publications of that journal in the two prior years. Learn more

515 total citable items

	ARTICLES	REVIEWS	COMBINED(C)	OTHER DOCUMENT TYPES(O)	PERCENTAG
NUMBER IN JCR YEAR 2024 (A)	477	38	515	14	97%
NUMBER OF REFERENCES (B)	21,655	3,202	24,857	14	100%
RATIO (B/A)	45.4	84.3	48.3	1.0	

The Average Journal Impact Factor Percentile takes the sum of the JIF Percentile rank for each category under consideration, then calculates the average of those values. Learn more

ALL CATEGORIES AVERAGE
55.8

CHEMISTRY, ANALYTICAL
59.9

BIOCHEMICAL RESEARCH METHODS
63.4

CHEMISTRY, PHYSICAL
44.1

Contributions by organizations

Export

Organizations that have contributed the most papers to the journal in the most recent three-year period. Learn more

RANK	ORGANIZATION	COUNT
1	EGYPTIAN KNOWLEDGE BANK (EKB)	64
2	NATIONAL INSTITUTE OF TECHNOLOGY (NIT SYSTEM)	44
3	KING SAUD UNIVERSITY	41
4	PUNJABI UNIVERSITY	20
5	MAHARSHI DAYANAND UNIVERSITY	18
6	INDIAN INSTITUTE	17

Contributions by country/region

Export

Countries or Regions that have contributed the most papers to the journal in the most recent three-year period. Learn more

RANK	COUNTRY / REGION	COUNT
1	INDIA	418
2	CHINA MAINLAND	387
3	EGYPT	67
4	IRAN	62
-	SAUDI ARABIA	62
6	PAKISTAN	59
7	TURKIYE	58
8	IRAQ	31
-	SOUTH KOREA	31

Additional metrics

Eigenfactor Score

0.00314

The Eigenfactor Score is a reflection of the density of the network of citations around the journal using 5 years of

Normalized Eigenfactor

0.70377

The Normalized Eigenfactor Score is the Eigenfactor score normalized, by rescaling the total number of journals

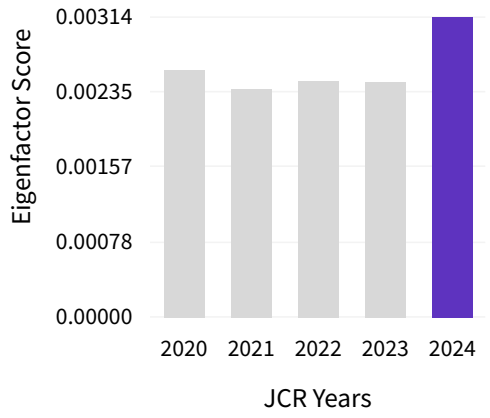
Article influence score

0.330

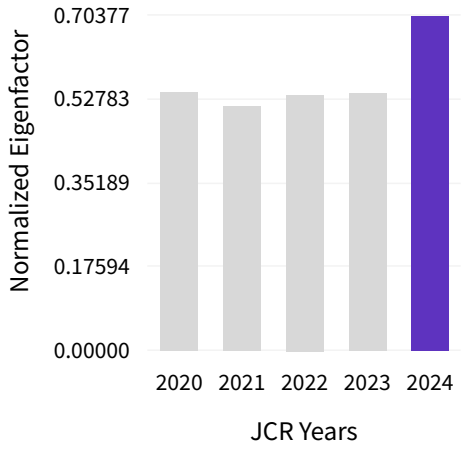
The Article Influence Score normalizes the Eigenfactor Score according to the cumulative size of the cited journal

15

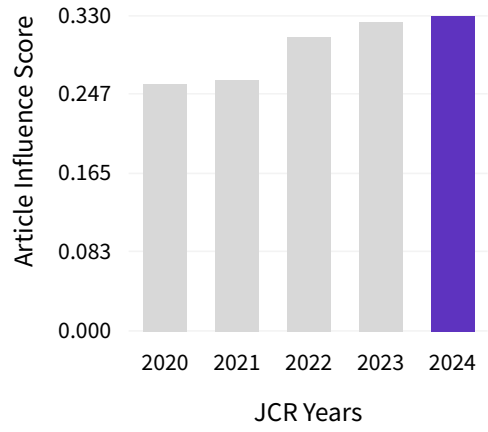
cited content as cited by the Current Year. It considers both the number of citations and the source of those citations, so that highly cited sources will influence the network more than less cited sources. The Eigenfactor calculation does not include journal self-citations. Learn more



in the JCR each year, so that the average journal has a score of 1. Journals can then be compared and influence measured by their score relative to 1. Learn more



across the prior five years. The mean Article Influence Score for each article is 1.00. A score greater than 1.00 indicates that each article in the journal has above-average influence. Learn more

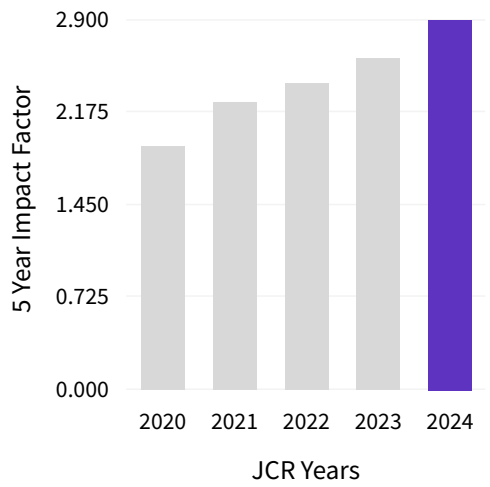


5 Year Impact Factor

2.9

View Calculation

The 5-year Impact Factor is the average number of times articles from the journal published in the past five years have been cited in the JCR year. It is calculated by dividing the number of citations in the JCR year by the total number of articles published in the five previous years. Learn more

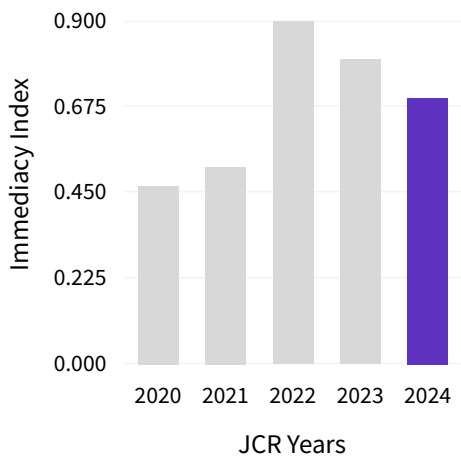


Immediacy Index

0.7

View Calculation

The Immediacy Index is the count of citations in the current year to the journal that reference content in this same year. Journals that have a consistently high Immediacy Index attract citations rapidly. Learn more



© 2025 Clarivate

Legal center

Privacy notice

Cookie policy

Terms of Use

Manage cookie preferences

Copyright notice

Accessibility

Help

15

SPRINGER NATURE Link

Log in

Menu Search Cart

Home > Journal of Fluorescence > Editorial board



Journal of Fluorescence
Publishing model: Hybrid

Kocaeli Üniversitesi Explore open access funding | Change institution

Journal menu

Editorial board

Editor-in-Chief

Chris D. Geddes, FRSC, PhD, University of Maryland Baltimore County, Baltimore, MD, United States of America

Columbus Center, 701 East Pratt St., Baltimore, MD, 21202

Associate Editors

Professor Robert M. Strongin, PhD, Portland State University, Portland, OR, USA.

Haishi Cao, PhD, Department of Chemistry, University of Nebraska at Kearney, Kearney, NE, United States of America

Regional Editor for Europe

Prof. Alan G. Ryder, PhD., University of Galway, Galway, Ireland.

Regional Editor for India

Professor Hirdyesh Mishra, PhD, Banaras Hindu University, Varanasi, India.

Regional Editor for Asia

Vladislav Papper, PhD, Ateneo de Davao University, Philippines.

Editorial Board

Professor Dipak Kumar Palit, Ph. D, UM-DAE Centre for Excellence in Basic Sciences, Mumbai, India.

Professor Christopher J. Abelt, Ph.D, William & Mary, Williamsburg, United States of America

Professor Jefferson Luis Ferrari, PhD, Institute of Chemistry, Uberlândia Federal University, Brazil

Professor Raju Nandhakumar, PhD, Karunya Institute of Technology and Sciences, Coimbatore, TamilNadu, India.

Professor Kate Grudpan, Ph.D, Chiang Mai university, Chiang Mai, Thailand

Dr. Giriyapura Prabhukumara Darshan, Ph.D, M S Ramaiah University of Applied Sciences, Ramaiah Technology Campus, Bengaluru, India

Professor George Barisas, Ph.D, Colorado State University, Fort Collins, CO, United States of America

Professor, Kevin Belfield, PhD, New Jersey Institute of Technology, United States of America

Professor Michael D. Heagy, Ph.D, Rochester Institute of Technology, United States of America

Professor Richard Thompson, Ph.D, University of Maryland School of Medicine, Maryland, United States of America



Journal of Fluorescence (2025) 35:2121–2133
https://doi.org/10.1007/s10895-023-03498-4

RESEARCH

GFP Transfection Alters Protein Expression Patterns in Prostate Cancer Cells: A Proteomic Study

Sevinc Yanar[1,2] · Mehmet Sarihan[1] · Murat Kasap[1] · Gurler Akpinar[1] · Kerem Teke[3] · Busra Yaprak Bayrak[4]

Received: 7 September 2023 / Accepted: 6 November 2023 / Published online: 19 March 2024
© The Author(s), under exclusive licence to Springer Science+Business Media, LLC, part of Springer Nature 2024

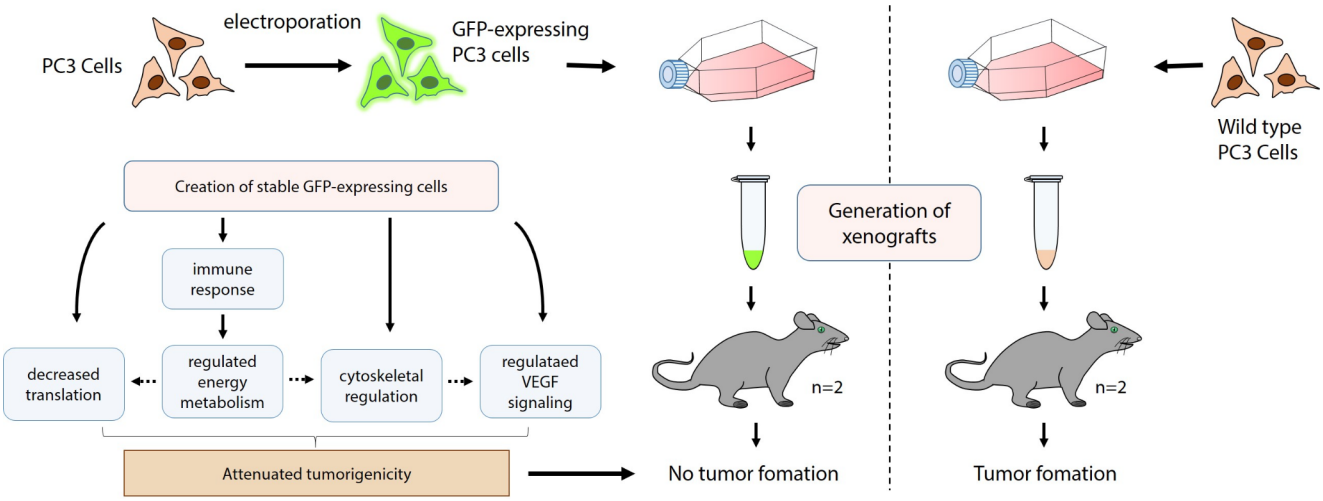
Abstract

Purpose Green Fluorescent Protein is widely used as a cellular marker tool, but its potential influence on cells has been questioned. Although the potential off-target effects of GFP on tumor cells have been studied to some extent, the findings at the molecular level are insufficient to explain the effect of GFP expression on the tumorigenic capacity of cancer cells. Here, we aimed to investigate the effect of GFP expression on the tumorigenicity of PC3 prostate cancer cells.

Methods Using GFP-expressing and wild-type PC-3 cells, xenograft models were generated in athymic BALB/C mice. To identify differentially expressed proteins, the change in cells proteome was investigated by label-free quantification with nano-high performance liquid chromatography to tandem mass spectrometry (nHPLC-MS/MS). Proteins that showed significantly altered expression levels were evaluated using the bioinformatics tools.

Results Unlike the wild-type PC-3 cells, GFP-expressing cells failed to develop tumor. Comparative proteome analysis of GFP-expressing cells with WT PC-3 cells revealed a total of 216 differentially regulated proteins, of which 98 were upregulated and 117 were downregulated.

Conclusion Upon GFP expression, differential changes in several pathways including the immune system, translational machinery, energy metabolism, elements of cytoskeletal and VEGF signaling pathway were observed. Therefore, care should be taken into account to prevent reporting deceitful mechanisms generated from studies utilizing GFP.



Keywords Green Fluorescent Protein · Prostate cancer · Tumorigenicity · Xenograft Model · Proteomics

Extended author information available on the last page of the article

Introduction

Green Fluorescent Protein (GFP) is an important tool as a cellular marker since the time it was used for in vivo imaging of cancer cells growing in athymic nude mice [1]. Researchers now have a better way to visualize gene expression and monitor cells thanks to the use of fluorescent proteins like GFP, which allow direct imaging of cells in vivo [2]. Imaging of GFP under a simple fluorescence microscope helped extensive characterization of protein expression patterns in cancer cells. The creation of cancer cells that stably express GFP and their transplantation into model organisms helped to image living cancer cells in their natural microenvironment. By this way, cancer cell trafficking in lymphatic channels, cancer neurogenesis, metastasis, cancer cell clonality, circulating tumor cells, and the efficacy of therapies have been successfully studied [2–4]. Despite its advantages, increasing evidence suggests that GFP can have debilitating effects on cells [5]. For example, interactions between GFP and other cellular proteins can cause a decrease in cell growth due to an increase in the amount of reactive oxygen species, which can lead to the activation of apoptotic cascades [6, 7]. Furthermore, at the tissue level, expression of GFP in muscle cells was associated with impaired contraction [8]. Similarly, the expression of GFP in cardiomyocytes caused cardiomyopathy in mice [9]. Interestingly, expression of EGFP, a GFP variant, in neurons induced apoptotic cell death and caused neurogenic paresis [10]. Also in neuroblastoma cells, transduction of GFP enhanced sensitivity to anti-tumor drugs causing intervention in cellular responses to therapeutics [11].

GFP expression can affect the tumorigenic potential of cancer cells. This effect was observed when intravenous injection of non-modified BM185 cells induced systemic leukemia and death of immunocompetent mice, but not the BM185-eGFP cells [12]. When immunodeficient mice were injected with eGFP-expressing cells, it resulted in death. In another study, mouse EL-4 lymphoma cells expressing eGFP did not propagate after subcutaneous injection to immunocompetent mice, unlike the parental cell line [13]. Comparison of different mouse tumor cell lines expressing fluorescent proteins resulted in varying tumorigenic capacity. Subcutaneous injection of GFP expressing 4T1 and B16-F10 cells had no effect on the tumor growth rate, while both CT26-GFP and CT26-RFP cells were rejected after implantation [14].

Despite definitive consequences of GFP expression on growth and cell metabolism, not much effort was placed on understanding the details of changes occurring at the molecular level upon GFP expression. Only a few studies examined this issue in cultured cells. For instance, GFP was shown to selectively induce HSP70 expression which resulted in the up-regulation of COX-2 expression in endothelial cells [15]. Also, GFP expression inhibited polyubiquitination causing derogatory effects on proteasome machinery [16]. The analysis of the transcriptional profile of cardiomyocytes expressing GFP indicated regulations in processes including responses to stimuli and signal transduction [17]. Investigation of the proteome modifications of GFP-expressing breast cancer cells showed changes in the expression profiles of proteins that are associated with cellular immune response, protein folding, and cytoskeletal organization [18]. Despite these reports, comprehensive studies investigating the proteome changes caused by GFP expression in in vivo are still lacking. The relationship of the revealed mechanisms with tumorigenicity has yet to be clarified as well. Therefore, in this study, we investigated the effects of GFP expression on the tumorigenicity of prostate cancer cells using proteomic approaches in a xenograft model.

Materials and Methods

Cell Culture

The human prostate cancer cell line PC-3 was purchased from the American Type Culture Collection (ATCC, Rockville, MD, USA). The cells were grown in Roswell Park Memorial Institute-1640 medium (RPMI-1640, Thermo Fisher Scientific, MA, USA) containing high glucose, supplemented with 10% fetal bovine serum (FBS) and 100 U/mL penicillin, and 100 µg/mL streptomycin. The cultures were maintained at 37 °C in a humidified incubator with 5% CO_2.

Creation of Stable PC-3 Cells Expressing GFP

PC-3 cells were transfected with pcDNA4/TO harboring the GFP gene using Neon transfection system (Thermofisher, USA) to create a stable cell line expressing high levels of GFP protein. Transfected cells were then subjected to selection in RPMI containing 50 µg/ml zeocin. To obtain monoclonal clones, separate colonies formed on the culture plates were picked with cloning cylinders and gradually propagated in 96-well culture plates. They were then transferred into 5 ml culture plates to which coverslips were added for visualization of GFP expression by immunofluorescence microscopy using Olympus CKX41 inverted fluorescence microscope (Olympus, Japan). One of the screened colonies expressing GFP was propagated and frozen for use in subsequent experiments.

Analysis of Cell Growth and Morphology

The growth rate of GFP-transfected cells and wild-type cells was investigated through viability assays, and their morphology was examined via microscopy imaging. Cell viability was determined using a trypan blue exclusion assay. In brief, cells were seeded on 6-well culture plates at a density of 2×10^5 cells per well. After adherence, at the end of 24, 48, and 72 h of the incubation period, cells harvested in PBS were mixed with trypan blue solution. Live and dead cells in the mixed solution were counted using a hemocytometer. Experiments were conducted in triplicate.

Animals and Generation of Xenograft Models

7–8 weeks-old male athymic (nude) BALB/C mice (n = 10) and GFP expressing (GFP+) and wild-type PC-3 (GFP-) cells were used in in vivo experiments. Animals were kept under pathogen-free standard laboratory conditions with a 12-hour light/dark cycle. Food and water were available *ad libitum*. Experiments were carried out in compliance with the Regulation of Animal Research Ethics Committee in Turkey. Ethical approval (KOU HADYEK 8/2-2019) was granted by Kocaeli University Animal Research Ethics Committee (Kocaeli, Turkey). The mice were divided into 5 groups with 2 mice in each group as follows: control (saline-injected), subcutaneously GFP + cells injected, subcutaneously GFP- cells injected, intraprostatic GFP + cells injected, and intraprostatic GFP- cells injected. Intraprostatic injections of 7.5×10^5 cells in PBS were performed to the dorsal prostate tissues of mice, as described in previously published reports [19, 20]. For subcutaneous injections, 5×10^6 cells suspended in PBS from each group were mixed with matrigel (Corning, USA) and injected into the left lumbar region of designated groups under anesthesia. The mice were sacrificed by the end of the second month and the bladder, prostate, seminal vesicles, and rectum were collected and fixed in 10% formalin. The pelvic region, where the prostate tissue is located, kidney, vertebra, lung, and liver were examined macroscopically for possible metastatic involvement. Those tissues were also examined microscopically after staining with hematoxylin and eosin to identify wild-type and GFP-expressing PC-3 cells using light- and fluorescence-microscopy, respectively.

Preparation of Protein Extracts and Sample Pools

Protein isolation was carried out as described in our previous study [21]. In our experimental setup, each "sample" corresponds to the cell-free extract obtained from one culture plate, whether it contained wild-type (WT) or GFP-expressing PC-3 cells. For comparing these two groups (WT or GFP-expressing) we utilized a total of three culture plates for each group. To start isolation, briefly, GFP expressing and wild-type PC-3 cells were washed with washing buffer (250 mM Sucrose containing Tris-HCl at pH 7.2) and then suspended in lysis buffer (8 M urea, 2 M thiourea, 4% CHAPS, 30 mM Tris pH 8.5, and protease inhibitor cocktail). They were then lysed in a mechanical disruption device using 0.2 mm stainless-steel beads (Bullet Blender; Next Advance, Troy, NY). After centrifugation, supernatants containing soluble proteins were obtained. Protein concentrations were measured using Bradford protein dye-binding assay (Bio-Rad, USA). Equal amounts of proteins from each of the three samples per group were combined into single tubes and protein concentrations were re-measured using the Qubit protein assay kit (Thermo Fisher Scientific) according to the manufacturer's protocol.

Protein Digestion and Identification by nLC-MS/MS

Proteins were digested using an in-solution tryptic digestion kit according to the manufacturer's instructions (Thermo Fisher, MA, USA). To ensure the robustness and reliability of our proteomic analysis, we performed three independent replicates for each group. This involved conducting three separate tryptic digestions and subsequent analyses for both the wild-type and GFP-expressing cell groups. Digested peptides were analyzed by nLC-MS/MS using an Ultimate 3000 RSLC nanosystem (Dionex, Thermo Fisher Scientific, USA) coupled to a Q Exactive mass spectrometer (Thermo Fisher Scientific USA). The entire system was controlled by Xcalibur 4.0 software (Thermo Fisher Scientific). After preconcentration and desalting of peptides on the trap column, they were transferred to a C18 reversed-phase analytical column (Acclaim PepMap RSLC 75 µmx15 cmx2 µm, 100 A diameter, Thermo Fisher Scientific, USA) for separation using a linear solvent gradient. The separation was executed using mobile phases A (0.1% formic acid in water) and B (80% acetonitrile and 0.05% Trifluoroacetic acid (TFA) in water). The gradient was 6–10% B in 70 min, 10–30% B in 150 min, 30–50% B in 40 min, 50–90% B in 20 min, 90% in 10 min, and 90–6% B in 10 min with ta flow rate of 300 nL/min. The data-dependent acquisition was performed with an MS scan mass window set at 400–2000 m/z and by selecting the top ten precursor ions. The full scan MS spectra were collected with a resolution of 70.000, thescan range of 400–2000 m/z, target automatic gain control of 3×10^6 ions, maximum injection time of 60 ms and spray voltage of 2.3 kV. Raw data were analyzed with Proteome Discoverer SEQUEST (version 2.2; Thermo Fisher Scientific) software. The following parameters were used for protein identification: peptide mass tolerance 10 ppm, MS/MS mass tolerance 0.2 Da, mass accuracy 2 ppm,

tolerant miscarriage 1, minimum peptide length 6 amino acids, fixed changes: cysteine carbamidomethylation, variable changes: methionine oxidation, and asparagine deamination. The data were then searched against the Uniprot/Swissprot database for protein identification. Label-free quantification was performed with Proteome Discoverer 2.2 (Thermo Fisher, USA) by the following filters: Peptide and protein identifications were accepted if their probability were greater than 95 and 99%, respectively, and included two or more identified peptides. The proteins which were identified in all three replicates were reported. The target false discovery rate (FDR) threshold (strict) was set as 0.01 and target FDR (relaxed) was set as 0.05 using Percolator node. The proteins whose quantitation was significantly different between the two groups were defined as differentially regulated proteins (DRPs). If the fold was more than 2, it was accepted as upregulated and if it was less than 0.5, it was accepted as downregulated ($p < 0.05$).

Western Blotting

25 µg of protein from each group was separated by 12% SDS-PAGE and transferred to a nitrocellulose membrane as described by Bal Albayrak [22]. Briefly, after the membrane was blocked in nonfat powdered milk in tris buffered saline, it was incubated with anti-vimentin (sc-373,717, Santa Cruz) and anti-β-actin (sc-81,178, Santa Cruz) antibodies overnight at 4 °C. β-actin was used as internal control to ensure equal protein loading. The membrane was washed three times with TBS-T and then incubated with HRP-labelled secondary antibody (Bio-Rad, USA) for 1 h at room temperature. Two separate Western blot analyses were conducted, and protein bands were visualized using an enhanced chemiluminescence detection system. Band intensities were measured three times independently. Regulatory changes and statistical analyses were performed using a total of six values for each band, and the results of the statistical analyses were presented as mean and standard deviation (Mean ± SD).

Bioinformatics Analysis

Classification of proteins was performed by using Protein ANalysis THrough Evolutionary Relationships (PANTHER, pantherdb.org) database. The identified differentially regulated proteins (DRPs) with Uniprot accession numbers were uploaded. The organism was specified as *Homo sapiens* and the following ontologies were selected: molecular function, biological process, cellular function, cellular component, protein class, and pathway. Protein-protein interactions were predicted by further analysis using Search Tool for the Retrieval of Interacting Genes/Proteins (STRING, https://string-db.org). The parameters for STRING search included an interaction score of medium confidence, no interactors for the first and second shells, active interaction sources of text mining, experiments, databases, co-expression, neighborhood, gene fusion and co-occurrence. The hits considered in this study had FDR smaller than 1e-05. The results were downloaded as bitmap images and images were recreated by Adobe Illustrator Version 6.

Statistical Analysis

The statistical analysis of the measured data and related graphic representations were performed by using GraphPad Prism 9.1.0 (La Jolla, CA, ABD). Vimentin levels among the groups and the nLC-MS/MS results were analyzed by one-way analysis of variance (ANOVA) followed by Tukey's test. P values less than 0,05 were considered statistically significant. In nLC-MS/MS analysis, total peak intensity values were used for normalization of the samples, and statistical analyses were performed using the tools in the Protein Discoverer 2.2 program. A background-based ANOVA test for ion quantification and utilized the Pairwise Ratio approach for inter-group comparisons were employed.

Results

Stable PC-3 Cells Expressing GFP

PC3 cells were transfected with pCDNA4/TO and selected with zeocin to generate a monoclonal cell line that expresses GFP at a high level. From 10 different clones, the colony with the highest GFP expression was selected for in vitro and in vivo experiments. Analysis of the images revealed that GFP expression in the cells appeared uniform, indicating a relatively consistent level of expression in each cell examined, thus verifying the monoclonality of the generated cell line. Close up examination of the cells, however, showed minor differences in cytoplasmic fluorescence intensities among the cells (Fig. 1).

Alteration in Cell Growth and Morphology

Expression of GFP protein caused a decrease in the number of viable cells in cultures. After 72 h of incubation, the effect on viability was more pronounced as many dead floating cells were also observable under a microscope. In addition, morphological analysis of the cells under a microscope revealed the presence of apoptotic cells, displaying bubble-like protrusions and smaller apoptotic bodies. Analysis of the trypan blue exclusion assay results indicated that prolonged incubation caused gradual loss of more of the

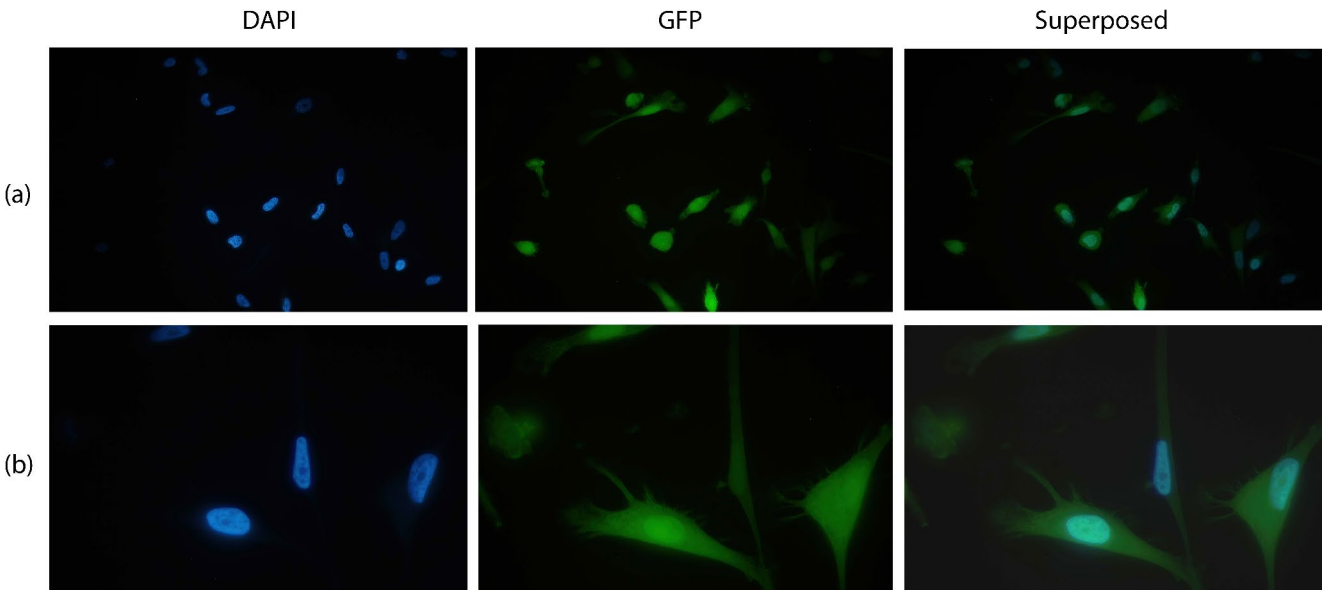


Fig. 1 PC3 cells stably expressing GFP. The nuclei were stained with DAPI, represented with blue color (**a**) 40x, (**b**) 100x magnification

GFP-expressing cells, which provided a statistically meaningful data showing decrease in cell number in time (Fig. 2).

Macroscopic and Microscopic Examination of Tissue Samples

Macroscopic and microscopic examinations revealed the absence of tumor development at the injection sites in both mice injected subcutaneously (n = 2) and intraprostatically (n = 2) with GFP + cells (Fig. 3a and b). Examination under a fluorescence microscope did not reveal the presence of GFP + cells in the injection sites of none of the mice. However, careful macroscopic examination revealed that 5 × 5 mm^2 solid nodules were present in the left lumbar regions of mice injected subcutaneously with WT PC-3 cells and that there were irregular appearances in seminal vesicles and prostate tissues of mice injected intraprostatically GFP- cells.

Microscopically, Gleason pattern 5 adenocarcinoma cells, exhibiting enlarged nuclear morphology and aggressive cell fragments, were visualized in the subcutaneous nodules and the dorsal prostate tissues of mice injected with WT PC-3 cells (Fig. 4a and b). Normal prostate and inflamed seminal vesicular tissues from control mice were examined. No apparent macroscopic abnormality was noted in the pelvis, kidney, vertebrae, lung, and liver.

Comparative Proteome Analysis of the Wild-type and GFP-expressing PC-3 Cells

The effects of stable GFP expression on PC-3 cells were analyzed using the changes in global protein expression profiles. Digested proteins from each group were analyzed by nHPLC coupled to LC-MS/MS and label-free quantification was performed to identify DRPs. 731 proteins were identified in the wild-type PC-3 cells, while only 642 proteins were identified in the GFP-expressing PC3 cells. 121 of the identified proteins were expressed only in the wild-type cells while 32 of them were expressed only in the GFP-expressing cells. The number of proteins shared by both groups was 610 as depicted in the Venn diagram (Fig. 5). Analysis of the shared proteins showed that there were 418 DRPs between the two groups, of which 164 and 254 were up- and downregulated, respectively, with greater than two-fold of change. When the results were filtered further using additional criterion such as identification by a minimum of two or more unique peptides, the numbers were reduced to 98 for the upregulated and 117 for the downregulated proteins making a total of 216 DRPs. The complete list of the identified proteins was presented in Supplementary 1.

Bioinformatics Analysis of Differentially Regulated Proteins

Bioinformatic analyzes were performed to associate DRPs with protein networks and molecular pathways. The PANTHER analysis showed that most of these proteins have binding and catalytic activity as their prominent molecular functions. The PANTHER classification to determine protein classes indicated that the expression profile of eighteen different protein types, specifically cytoskeletal proteins (including P08670, P26038, P07437, Q9UHD8, Q16658), translational proteins (including P46781, P40429, P62277, P62906, P25398) and metabolite interconversion enzymes

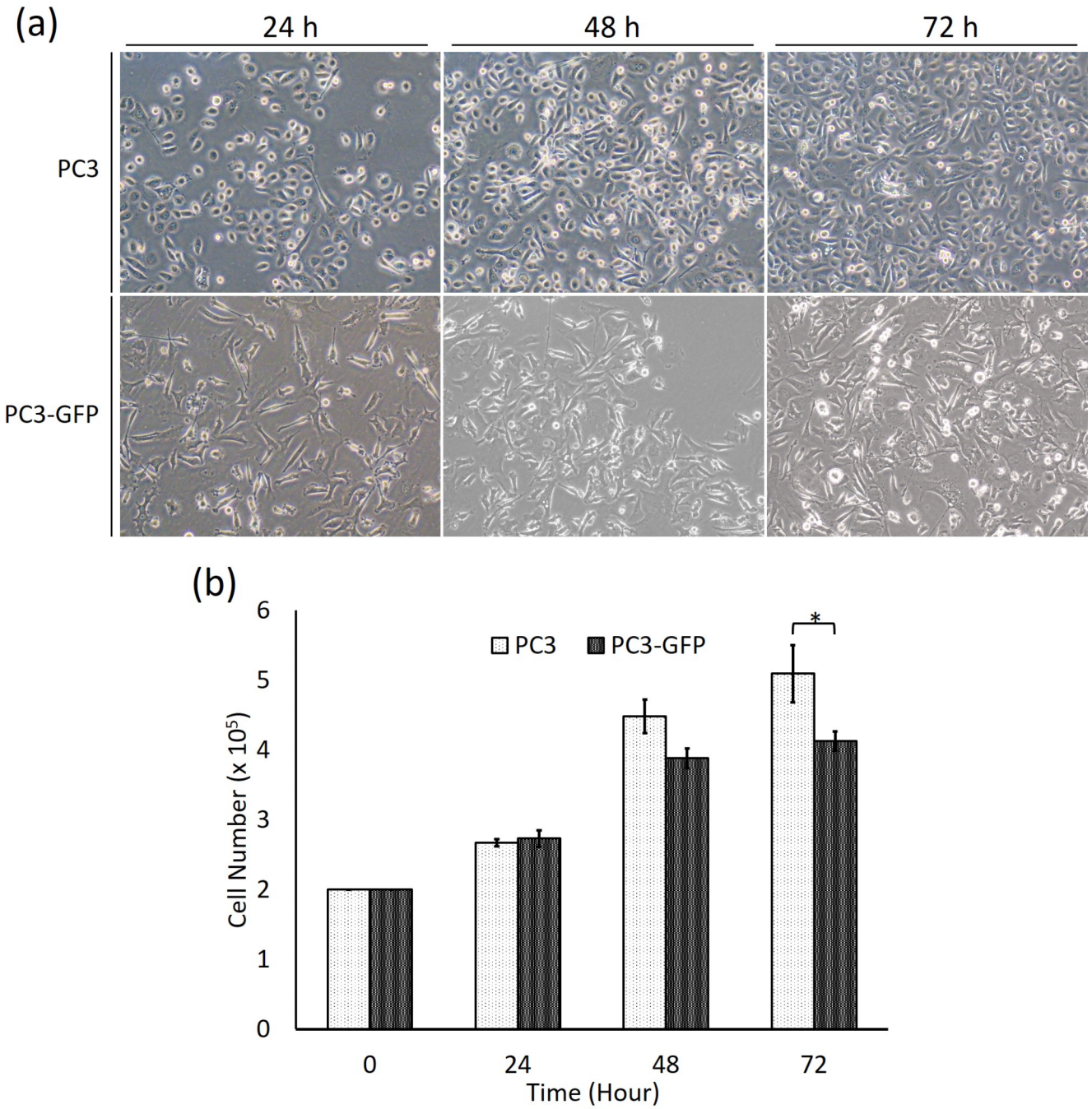


Fig. 2 (**a**) Inverted microscopy images of WT-PC3 and GFP-expressing cells after 24, 48 and 72 h of incubation. (**b**) Bar graph for presentation of trypan-blue exclusion assay for analysis of cell viability after 24, 48 and 72 h of incubation (*$P < 0.05$)

were altered. Pathway analysis by PANTHER drew attention to cytoskeletal regulation, glycolysis (P04406, P00558, P18669, P14618), ATP synthesis, integrin signaling pathway (P00034), inflammation (O15144, P12109I, P35579), angiogenesis and VEGF signaling (P04792). Further bioinformatic analysis of DRPs by STRING showed that there were mainly regulations related to translation, immune response, glycolytic activity, Cori cycle, cell adhesion molecule binding, and VEGFA-VEGFR2 signaling (Fig. 6). The results of the STRING analysis showed high similarity to the PANTHER analysis. Thus, we can consider the key mechanisms altered by stable GFP expression in PC-3 cells as follows: immune response, translational activity, energy metabolism, cytoskeletal regulation, and VEGF signaling.

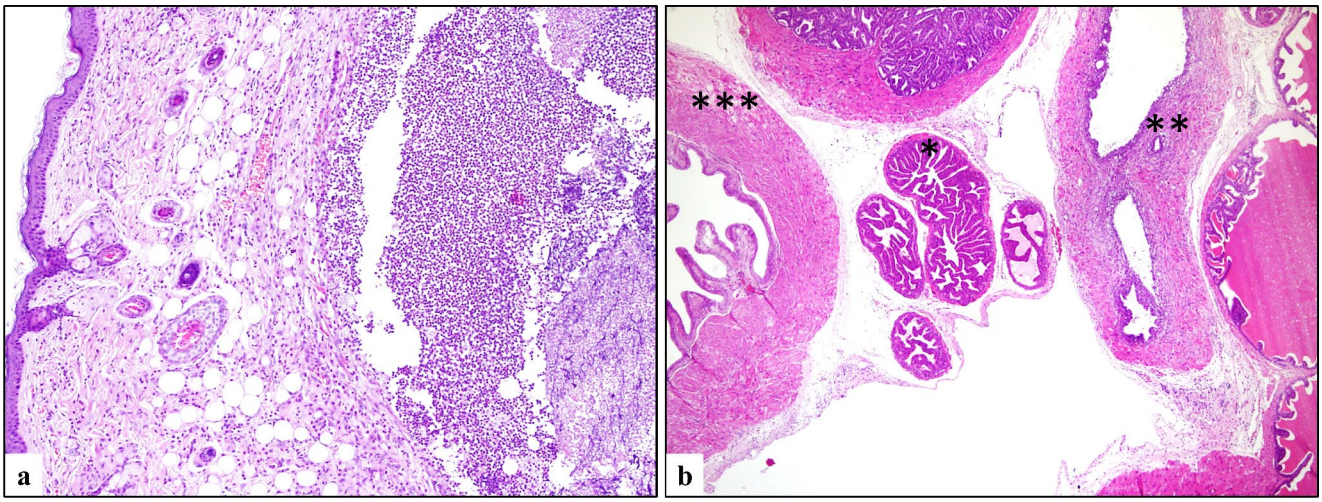


Fig. 3 Absence of GFP+cells in subcutaneous and intraprostatic injected tissues (**a**) Abscess formation in the subcutaneous mouse tissue (H&E, 40x); (**b**) * : normal prostate, **: seminal vesicle and ***: bladder tissue (H&E, 40x)

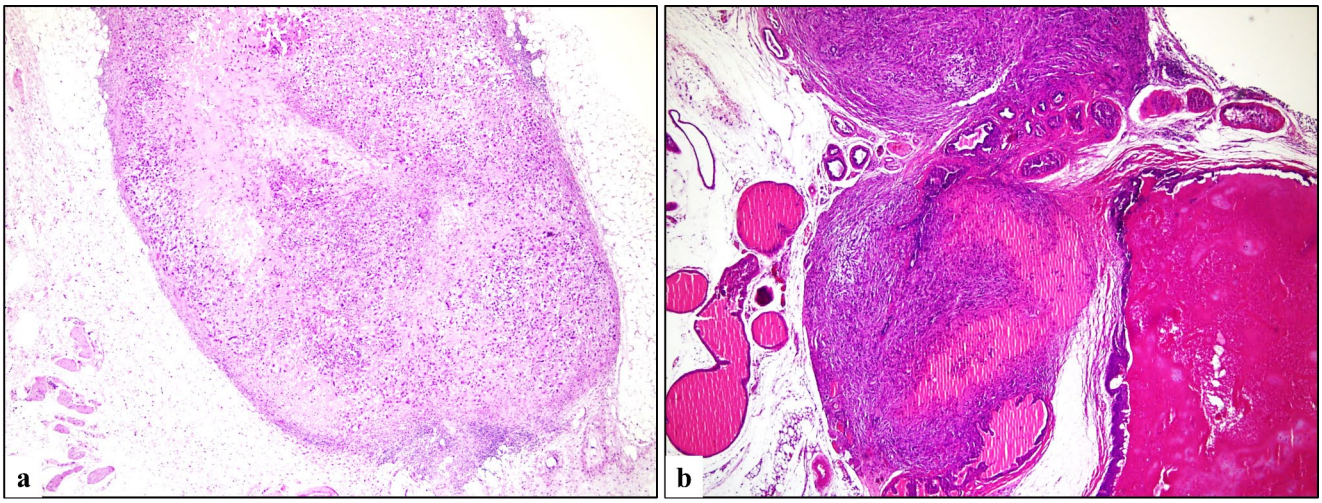


Fig. 4 Wild-type PC-3 cells in subcutaneous (**a**) and intraprostatic (**b**) injected tissues. (**a**) Tumor tissue with a nodular appearance in the surrounding muscle-fatty tissue of a mouse (H&E 40 x); (**b**) microscopic image from a mouse shows the wild-type PC-3 cells, which intertwined with normal prostate tissue (Gleason score 5 pattern) (H&E,40x)

Verification by Western Blotting

To confirm the results of the label-free quantification, a western blot analysis was performed for one of the differentially regulated proteins, vimentin. The expression level of vimentin increased significantly in GFP-expressing cells compared to the wild-type cells, consistent with the findings of label-free quantification (Fig. 7).

Discussion

Macroscopic and microscopic evaluation of xenograft models revealed the difference in tumorigenesis. Xenograft models created by wild-type cells, either by subcutaneously or intraprostatic injection, formed tumors whereas the models created by GFP-expressing cells did not. There are controversial reports in the literature about the tumorigenic potencies of GFP-expressing cells. Skelton et al. showed that non-modified BM185 leukemia cells induced systemic leukemia in immunocompetent mice while injection of BM185-eGFP did not. When immunodeficient mice were used, injection of eGFP-expressing cells resulted in leukemia [12]. The study of Stripecke et al. produced similar results; mouse EL-4 lymphoma cells expressing eGFP did not grow after subcutaneous injection to immunocompetent mice, unlike the parental cell line [13]. In another study, subcutaneous injection of GFP expressing 4T1 (murine breast cancer) and B16-F10 (murine melanoma) cells had no effect on the tumor growth rate, whereas CT26-GFP

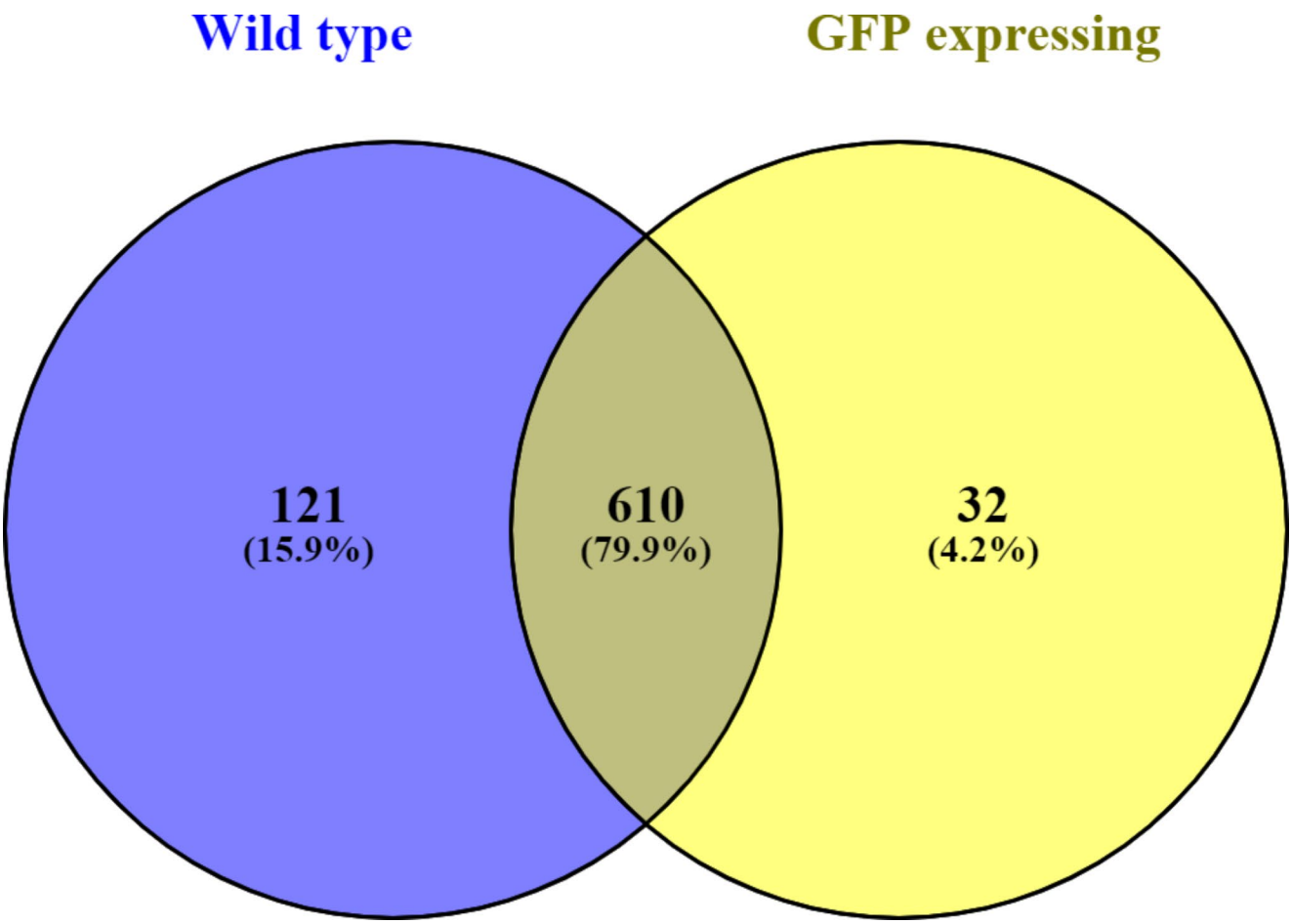


Fig. 5 A Venn diagram showing the number of proteins identified by nLC-MS/MS. A total of 763 different proteins were identified

(murine colon cancer) cells were rejected after implantation [14]. When the results of our xenograft study were evaluated together with the aforementioned studies, it is fair to say that the tumorigenic capacity of GFP-expressing cells varies regardless of the animal model or cell type used. We can assert that GFP-expressing PC3 cells might not be a suitable model for xenograft studies. The herein presented results of our proteomics study helped to elucidate the underlying mechanisms.

Regulation of immune response appeared one of the key altered mechanisms by GFP expression. Bioinformatics analysis by STRING directed our attention to upregulated proteins CSTB, CD44, Galectin 1, PKM2, PRDX6, and PSMC3 whose role has been identified in innate immunity. CSTB, a cysteine protease inhibitor, is thought to play important role in countering inflammation as well as in tumorigenesis [23]. CD44 was shown to mediate inflammatory cell recruitment, particularly leukocytes [24]. Its expression was reported to be important in the migration of prostate cancer cells [25]. While increased CD44 levels are often associated with cell proliferation, differentiation, and migration, the multifunctional nature of CD44 as a cell surface protein can lead to unforeseen effects on cells. This complexity in CD44's biology arises from extensive alternative splicing of the original transcript and diverse posttranslational modifications, resulting in numerous molecular isoforms with differing functions that are expressed differentially in various cell types [26]. Galectin 1 has been shown to modulate critical immunoregulatory molecules and their associated functions through a non-apoptotic ERK1/2-dependent pathway [27]. The effects of this protein on tumor growth are known to be multifaceted, depending on the cell type responding or its subcellular localization [28]. PKM2 was also found to have immunomodulatory effects [29]. Considering that PKM2 is involved in the glycolysis process and glucose is an instant source of energy for immune cells, PKM2 seems to have variable effects on immunity [29]. The antioxidant enzyme PRDX6 is a key regulator of the cellular redox balance, particularly under stress conditions. It has been shown to have a pivotal role in the defense of cellular oxidative stress and host immune responses [30]. Since the level of SOD protein was also remarkably elevated in the GFP-expressing group, the regulation of these two proteins could

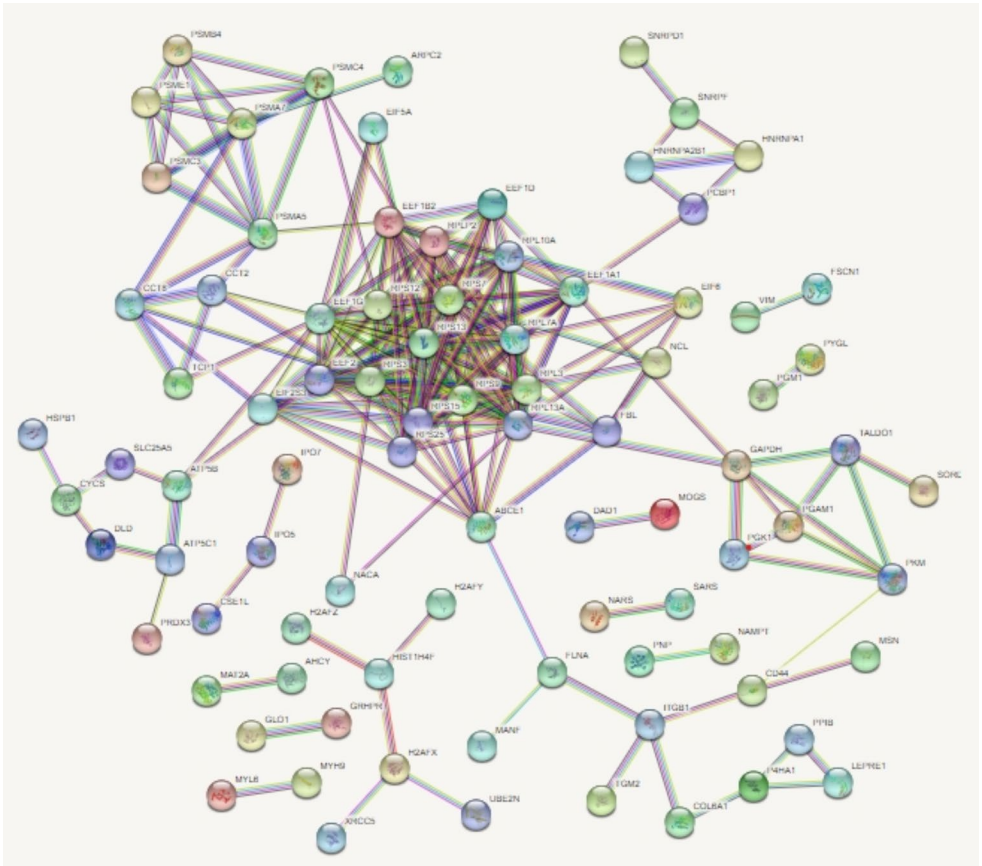


Fig. 6 An illustration of the protein network revealed by STRING analysis that shows how the differentially regulated proteins identified by nLC-MS/MS interact with each another

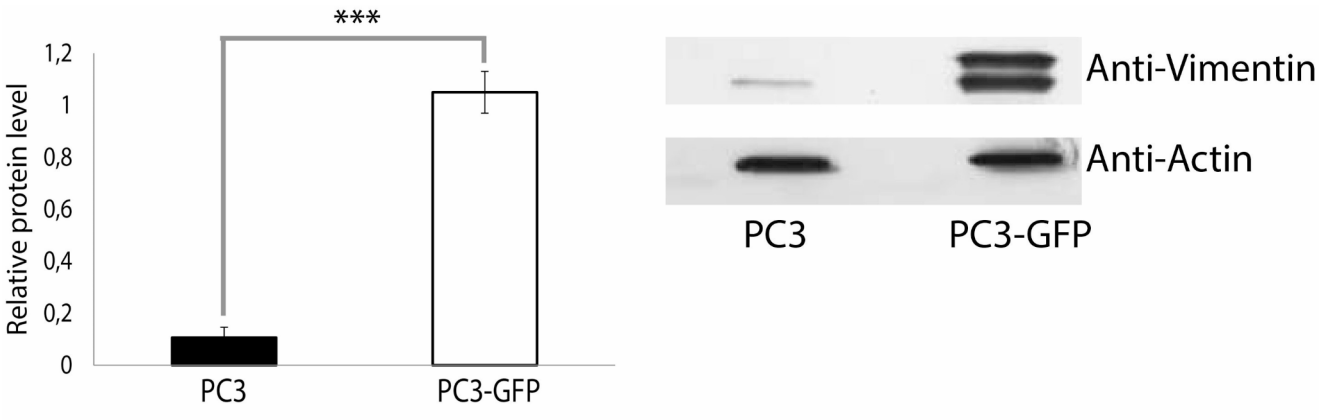


Fig. 7 Representative western blot image and relative expression level of vimentin protein (***$P < 0.001$)

be associated with the activation of the immune system in response to oxidative stress.

In their proteomics study, Coumans et al. showed that immune response was triggered as a consequence of GFP expression in breast cancer cells and they suggested that this was due to cellular stress [18]. However, their results could not elucidate the effects of altered immune response on the tumor-forming ability of cells. The results of our study imply that the above-mentioned proteins which are associated with altered immune response may have both directly or indirectly reduced tumorigenicity of GFP-expressing cells. While the existing studies in the literature, as explained above, can explain their direct effects [25, 28, 29], their indirect effects could be explained by the fact that the regulations in the immune system have effects on energy metabolism and the regulation of energy metabolism has a direct relation to tumorigenesis. The results of our proteomics study revealed regulation in proteins related to energy metabolism, mainly to glycolysis and Cori cycle. It is well known that the activation of immune response carries

a considerable bioenergetics cost [31]. Immune system cells secrete inflammatory mediators, cytokines, or chemokines in response to a stimulus. These responses can only be maintained if immune cells can sufficiently increase the uptake of nutrients like glucose from their microenvironment [31]. Since cancer cells have increased energy requirements compared to normal cells, cellular energy metabolism is an indispensable aspect of tumorigenesis [32]. Considering the findings collectively, a hypothesis emerges that deserves further investigation. It's possible that the immune response triggered by GFP expression could influence tumorigenicity, potentially by affecting cellular energy metabolism. However, it's important to note that we are not definitively establishing a direct cause-and-effect relationship between GFP expression and tumorigenicity. Instead, we are exploring potential mechanisms that may underlie the observed changes in protein expression.

Bioinformatics analyses highlighted the regulation of seven proteins (PKM, GAPDH, PGAM1, PGK1, PGM1, DLD, TALDO) associated with glycolysis. While six of them showed an increase in expression, only one (DLD) showed decreased expression pattern. These proteins pointed directly to the glycolytic pathway and thus to energy metabolism. Studies in the literature have demonstrated that some of these proteins, like PGK1 and PGM1, are associated with reduced tumorigenesis [33, 34]. Thus, their upregulation in GFP-expressing cells might have some adverse effects on tumorigenic capacity. Along with increased glycolytic proteins, the decrease in DLD expression level also draws attention to the disturbances in energy metabolism. The down-regulation of DLD has been shown to induce autophagic cell death in melanoma cells and inhibit in vivo tumor growth via triggering oxidative stress and altering energy metabolism [35]. Considering that some other proteins related to oxidative stress (PRDX6 and SOD) were also regulated, these findings point out that oxidative stress may have a role in the regulation of energy metabolism and immune response.

The upregulation of glycolysis-related proteins may also indicate an enhanced Warburg effect which is the consumption of more glucose and the production of higher amounts of lactate by cancer cells, even in a highly oxygenated environment [36]. Our findings reveal the involvement of key proteins (GAPDH, PGAM1, PKG1, TALDO) in the Cori cycle, a metabolic process associated with the Warburg effect in cancer cells. This suggests an increase in Cori cycle activity, supporting the notion of an enhanced Warburg effect as a response to stable GFP expression [37]. This indicates that cells are trying to rearrange their metabolism in order to survive the stress created by stable GFP expression. It seems plausible that an increase in immune response due to GFP expression has the potential to induce alterations in energy metabolism, which could be a part of the cellular survival system.

Energy metabolism can also indirectly affect tumorigenicity by causing regulations in translational activity [38] or cytoskeletal dynamics [39]. Bioinformatics analyses of our results highlighted twenty-six proteins related to translation, twenty of which were downregulated, including some key translational proteins such as EIF2,-5,-6 subunits, and EEF1 subunits. Therefore, it is tempting to speculate that translational activity was decreased in GPF-expressing cells. Among the identified proteins, eukaryotic initiation factors (EIFs) and their subunits attracted our attention for their significant correlation with many oncogenic processes in various types of cancers like breast, prostate, and colorectal cancer [38]. Since the overexpression of these proteins is associated with advanced tumor stage or poor prognosis, their downregulation in response to GFP expression may be a reason for the reduced tumorigenic capacity of cells. Translation is a pivotal step in the regulation of gene expression and is also one of the most energetically demanding processes in the cell. Dysregulation of translation results in abnormal gene expression like overexpression, downregulation, or phosphorylation and thus leads to uncontrolled cell growth potentially resulting in oncogenic progression [38]. Therefore, the regulation of translational proteins could be regarded as a prominent factor that affects the tumorigenic capacity of GFP-expressing cells. It could also be argued that counter-changes in translational proteins may provide a balance to the altered energy metabolism associated with GFP expression, thereby promoting cell survival but attenuating their tumorigenicity. Since translation is an energy-demanding process, cells may be conserving energy to adapt to changing conditions following GFP expression by decreasing the translation level of various proteins.

Another key altered mechanism upon GFP expression is cytoskeletal organization as implied by the downregulation of sixteen and upregulation of ten cytoskeletal proteins. Cell adhesion molecule binding, cadherin, and actin filament binding appeared to be the basic regulated functions. Coumans et al. suggested that the cytoskeletal structure, cell shape, and motility may be impacted by GFP expression in breast cancer cells [18]. It was also demonstrated that co-expression of eGFP and β-galactosidase in the cytoplasm of mouse forebrain neurons caused a contractile malfunction by interfering with the connections between actin and myosin in muscle cells [8, 10]. Beyond playing role in cellular shape, the cytoskeleton is also essential for controlling a number of cellular functions such as proliferation, transformation, and apoptosis [40]. Cellular tumorigenicity and changes in the cytoskeletal organization are found to be closely connected. Cancerous cells become softer as a result of significant alterations to the cell's structure, which

facilitates their uncontrolled growth and invasion [41]. Regulations in the cytoskeleton may be directly related to GFP expression or may be related to changes in energy metabolism since the regulation of the cytoskeleton is a significant expenditure of energy [39]. Cells modify their metabolism by altering glycolysis or oxidative phosphorylation and provide the energy required for cytoskeletal rearrangement that takes place during epithelial-to-mesenchymal transition, migration, and invasion [39]. When all these are evaluated as a whole, it is enticing to conclude that the rearrangement of the cytoskeleton is both directly connected to the expression of GFP or indirectly related to energy metabolism. Whether this was directly or indirectly, the cells became less tumorigenic as a result.

Our bioinformatics analysis had another striking outcome regarding vascular endothelial growth factor (VEGF) signaling (fdr: 8.72e-06). There were nine upregulated (NCL, RPLP2, ANXA1, RAB11A, MYH9, SARS, CYCS, PNP, CF11) and eight downregulated (RPL13A, RPL10A, ITGB1, FSCN1, GAPDH, PGK1, PRDX6, HSPB1) proteins pointing to the VEGFA/VEGFR2 signaling pathway. It is well known that this pathway serves as the main mediator of the cellular responses involved in angiogenesis, one of the key processes in tumorigenesis [42]. In addition to its principal expression on endothelial cells, VEGFR2 was found to be present on cancer cells in several cancers like breast, lung, gastrointestinal, ovarian, and bladder cancer, and therefore the regulation of the downstream pathway is regarded as a crucial factor in proliferation, migration, and invasion of tumor cells [43]. Hence, it is alluring to speculate that regulation of VEGFA/VEGFR2 signaling explains in part why GFP-expressing cells failed to develop tumors.

To confirm the results of the label-free quantification, a Western blot analysis was performed for vimentin, one of the differentially regulated proteins. The expression level of vimentin increased significantly in GFP-expressing cells compared to the wild-type cells, consistent with the findings of label-free quantification. This consistency underscores the reliability of our quantitative protein analysis.

When addressing the limitations of our study, the use of a single cell line representing aggressive prostate cancer restricts our ability to generalize our findings. Future experiments involving different cell lines from diverse cancer types will be crucial in understanding whether GFP expression affects these cell types in a similar manner, possibly through shared or distinct metabolic pathways. Furthermore, it's important to note that our study employed a limited number of biological and technical replicates in the animal experiments. This limitation arose from our initial plan to establish xenograft models with GFP-expressing cells. Unforeseen complications related to GFP expression hindering PC-3 cell proliferation prevented us from using a larger animal cohort, which was restricted for ethical reasons. Additionally, in our in vitro cell culture experiments, we employed pools created from cell-free extracts, assuming that these pools accurately represented the replicative cultures. While this method aligns with existing practices in the literature, it's worth noting that it does have implications. To capture individual variations and sample-specific changes, one could opt to perform comparative proteome analysis on each cell-free extract separately. However, individual analysis approach introduces increased analytical variability, as each sample necessitates its unique sample preparation and mass spectrometry steps. Handling a larger number of individual samples also adds complexity to data management and processing.

Conclusion

In conclusion, GFP-expressing PC3 cells failed to develop tumors in xenograft models. Using tools of proteomics and bioinformatics several differentially expressed proteins were identified in GFP-expressing cells as compared to wild-type cells. The most striking regulations were in immune response, translational activity, energy metabolism, cytoskeletal regulation, and VEGF signaling. Alterations in these mechanisms caused attenuated tumorigenicity either separately or by affecting each other. These findings point out that if GFP-expressing cells are to be used in in vivo studies, a comprehensive study investigating how the cells are affected by GFP is required. The study should be started by taking into account any circumstances that call for regulation, such as the usage of immunosuppressants or energy boosters. A different approach should be used instead of GFP if there is a risk that the study's findings can be misinterpreted.

Supplementary Information The online version contains supplementary material available at https://doi.org/10.1007/s10895-023-03498-4.

Authors' Contributions The study was designed by SY, MK and GA. Experiments, data collection and analysis were performed by SY, MK, MS, KT and BY. Data were interpreted by SY, MK and GA. The first draft of the manuscript was written by SY in consultation with MK and all authors commented on previous versions of the manuscript. All authors read and approved the final manuscript.

Funding The authors declare that no funds, grants, or other support were received during the preparation of this manuscript.

Data Availability Data are available on request from the authors.

Declarations

Ethics Approval This study was performed in compliance with the Regulation of Animal Research Ethics Committee in Turkey. Ethical approval (KOÜ HADYEK 8/2-2019) was granted by Kocaeli University Animal Research Ethics Committee (Kocaeli, Turkey).

Competing Interests The authors declare no competing interests.

References

1. Chishima T, Miyagi Y, Wang X, Yamaoka H, Shimada H, Moossa AR, Hoffman RM (1997) Cancer invasion and micrometastasis visualized in live tissue by green fluorescent protein expression. Cancer Res 57:2042–2047
2. Hoffman RM (2015) Application of GFP imaging in cancer. Lab Invest 95:432–452. https://doi.org/10.1038/labinvest.2014.154
3. Hoffman RM (2002) Green fluorescent protein imaging of tumour growth, Metastasis, and angiogenesis in mouse models. Lancet Oncol 3:546–556. https://doi.org/10.1016/s1470-2045(02)00848-3
4. Yamamoto N, Tsuchiya H, Hoffman RM (2011) Tumor imaging with multicolor fluorescent protein expression. Int J Clin Oncol 16:84–91. https://doi.org/10.1007/s10147-011-0201-y
5. Ansari AM, Ahmed AK, Matsangos AE, Lay F, Born LJ, Marti G, Harmon JW, Sun Z (2016) Cellular GFP toxicity and immunogenicity: potential confounders in in vivo cell tracking experiments. Stem Cell Rev Rep 12:553–559. https://doi.org/10.1007/s12015-016-9670-8
6. Taghizadeh RR, Sherley JL, CFP and, YFP, but Not GFP (2008) Provide stable fluorescent marking of rat hepatic adult stem cells. J Biomed Biotechnol 2008:453590. https://doi.org/10.1155/2008/453590
7. Gambotto A, Dworacki G, Cicinnati V, Kenniston T, Steitz J, Tüting T, Robbins P, DeLeo A (2000) Immunogenicity of enhanced green fluorescent protein (EGFP) in BALB/c mice: identification of an H2-Kd-restricted CTL epitope. Gene Ther 7:2036–2040. https://doi.org/10.1038/sj.gt.3301335
8. Agbulut O, Huet A, Niederländer N, Puceat M, Menasché P, Coirault C (2007) Green fluorescent protein impairs actin-myosin interactions by binding to the actin-binding site of Myosin*. J Biol Chem 282:10465–10471. https://doi.org/10.1074/jbc.m610418200
9. Huang W-Y, Aramburu J, Douglas PS, Izumo S (2000) Transgenic expression of green fluorescence protein can cause dilated cardiomyopathy. Nat Med 6:482–483. https://doi.org/10.1038/74914
10. Krestel HE, Mihaljevic ALA, Hoffman DA, Schneider A (2004) Neuronal co-expression of EGFP and β-galactosidase in mice causes neuropathology and premature death. Neurobiol Dis 17:310–318. https://doi.org/10.1016/j.nbd.2004.05.012
11. Goto H, Yang B, Petersen D, Pepper KA, Alfaro PA, Kohn DB, Reynolds CP (2003) Transduction of green fluorescent protein increased oxidative stress and enhanced sensitivity to cytotoxic Drugs in neuroblastoma cell lines. Mol Cancer Ther 2:911–917
12. Skelton D, Satake N, Kohn D (2001) The enhanced green fluorescent protein (eGFP) is minimally immunogenic in C57BL/6 mice, Gene Ther. 8:1813–1814. https://doi.org/10.1038/sj.gt.3301586
13. Stripecke R, Villacres MdelC, Skelton DC, Satake N, Halene S, Kohn DB (1999) Immune response to green fluorescent protein: implications for gene therapy. Gene Ther 6:1305–1312. https://doi.org/10.1038/sj.gt.3300951
14. Vodopyanov SS, Kunin MA, Garanina AS, Grinenko NF, Vlasova KY, Mel'nikov PA, Chekhonin VP, Sukhinich KK, Makarov AV, Naumenko VA, Abakumov MA, Majouga AG (2019) Preparation and Testing of Cells Expressing Fluorescent Proteins for Intravital Imaging of Tumor Microenvironment, B Exp Biol Med+. 167:123–130. https://doi.org/10.1007/s10517-019-04475-3
15. Zhang F, Hackett NR, Lam G, Cheng J, Pergolizzi R, Luo L, Shmelkov SV, Edelberg J, Crystal RG, Rafii S (2003) Green fluorescent protein selectively induces HSP70-mediated up-regulation of COX-2 expression in endothelial cells. Blood 102:2115–2121. https://doi.org/10.1182/blood-2003-01-0049
16. Baens M, Noels H, Broeckx V, Hagens S, Fevery S, Billiau AD, Vankelecom H, Marynen P (2006) The Dark side of EGFP: defective polyubiquitination. PLoS ONE 1:e54. https://doi.org/10.1371/journal.pone.0000054
17. Badrian B, Bogoyevitch MA (2007) Changes in the Transcriptional Profile of Cardiac myocytes following green fluorescent protein expression. Dna Cell Biol 26:727–736. https://doi.org/10.1089/dna.2007.0604
18. Coumans JVF, Gau D, Poljak A, Wasinger V, Roy P, Moens P (2014) Green fluorescent protein expression triggers proteome changes in Breast cancer cells. Exp Cell Res 320:33–45. https://doi.org/10.1016/j.yexcr.2013.07.019
19. Pang K, Xie C, Yang Z, Suo Y, Zhu X, Wei D, Weng X, Wei X, Gu Z (2018) Monitoring circulating Prostate cancer cells by in vivo flow cytometry assesses androgen deprivation therapy on Metastasis. Cytom Part A 93:517–524. https://doi.org/10.1002/cyto.a.23369
20. Shahryari V, Nip H, Saini S, Dar AA, Yamamura S, Mitsui Y, Colden M, Bucay N, Tabatabai LZ, Greene K, Deng G, Tanaka Y, Dahiya R, Majid S (2016) Pre-clinical orthotopic murine model of human Prostate Cancer. J Vis Exp. https://doi.org/10.3791/54125
21. Yanar S, Kasap M, Kanli A, Akpinar G, Sarihan M (2022) Proteomics analysis of meclofenamic acid-treated small cell lung carcinoma cells revealed changes in cellular energy metabolism for cancer cell survival. J Biochem Mol Toxicol e23289. https://doi.org/10.1002/jbt.23289
22. Albayrak MGB, Simsek T, Kasap M, Akpinar G, Canturk NZ, Guler SA (2022) Tissue proteome analysis revealed an association between cancer, immune system response, and the idiopathic granulomatous mastitis. Méd Oncol 39:238. https://doi.org/10.1007/s12032-022-01845-2
23. Ni J, Abrahamson M, Zhang M, Fernandez MA, Grubb A, Su J, Yu G-L, Li Y, Parmelee D, Xing L, Coleman TA, Gentz S, Thotakura R, Nguyen N, Hesselberg M, Gentz R (1997) Cystatin E is a Novel Human cysteine proteinase inhibitor with structural resemblance to family 2 Cystatins*. J Biol Chem 272:10853–10858. https://doi.org/10.1074/jbc.272.16.10853
24. Khan AI, Kerfoot SM, Heit B, Liu L, Andonegui G, Ruffell B, Johnson P, Kubes P (2004) Role of CD44 and Hyaluronan in Neutrophil Recruitment. J Immunol 173:7594–7601. https://doi.org/10.4049/jimmunol.173.12.7594
25. Desai B, Rogers MJ, Chellaiah MA (2007) Mechanisms of osteopontin and CD44 as metastatic principles in Prostate cancer cells. Mol Cancer 6:18. https://doi.org/10.1186/1476-4598-6-18
26. Azevedo R, Gaiteiro C, Peixoto A, Relvas-Santos M, Lima L, Santos LL, Ferreira JA (2018) CD44 glycoprotein in cancer: a molecular conundrum hampering clinical applications. Clin Proteom 15:22. https://doi.org/10.1186/s12014-018-9198-9
27. Barrionuevo P, Beigier-Bompadre M, Ilarregui JM, Toscano MA, Bianco GA, Isturiz MA, Rabinovich GA (2007) A novel function for Galectin-1 at the crossroad of Innate and adaptive immunity: Galectin-1 regulates Monocyte/Macrophage physiology through a nonapoptotic ERK-Dependent pathway. J Immunol 178:436–445. https://doi.org/10.4049/jimmunol.178.1.436
28. Rabinovich GA (2005) Galectin-1 as a potential cancer target. Brit J Cancer 92:1188–1192. https://doi.org/10.1038/sj.bjc.6602493

29. Gupta V, Bamezai RNK (2010) Human pyruvate kinase M2: a multifunctional protein. Protein Sci 19:2031–2044. https://doi.org/10.1002/pro.505
30. Priyathilaka TT, Kim Y, Udayantha HMV, Lee S, Herath HMLPB, Lakmal HHC, Elvitigala DAS, Umasuthan N, Godahewa GI, Kang SI, Jeong HB, Kim SK, Kim DJ, Lim BS (2016) Identification and molecular characterization of peroxiredoxin 6 from Japanese eel (Anguilla japonica) revealing its potent antioxidant properties and putative immune relevancy. Fish Shellfish Immun 51:291–302. https://doi.org/10.1016/j.fsi.2015.12.012
31. Ganeshan K, Chawla A (2014) Metabolic regulation of Immune responses. Annu Rev Immunol 32:609–634. https://doi.org/10.1146/annurev-immunol-032713-120236
32. Neagu M, Constantin C, Popescu ID, Zipeto D, Tzanakakis G, Nikitovic D, Fenga C, Stratakis CA, Spandidos DA, Tsatsakis AM (2019) Inflammation and metabolism in Cancer Cell—Mitochondria Key Player. Front Oncol 9:348. https://doi.org/10.3389/fonc.2019.00348
33. He Y, Luo Y, Zhang D, Wang X, Zhang P, Li H, Ejaz S, Liang S (2019) PGK1-mediated cancer progression and drug resistance. Am J Cancer Res 9:2280–2302
34. Jin G-Z, Zhang Y, Cong W-M, Wu X, Wang X, Wu S, Wang S, Zhou W, Yuan S, Gao H, Yu G, Yang W (2018) Phosphoglucomutase 1 inhibits hepatocellular carcinoma progression by regulating glucose trafficking. Plos Biol 16:e2006483. https://doi.org/10.1371/journal.pbio.2006483
35. Yumnam S, Kang MC, Oh SH, Kwon HC, Kim JC, Jung ES, Lee CH, Lee A-Y, Hwang J-I, Kim SY (2021) Downregulation of dihydrolipoyl dehydrogenase by UVA suppresses Melanoma progression via triggering oxidative stress and altering energy metabolism. Free Radical Bio Med 162:77–87. https://doi.org/10.1016/j.freeradbiomed.2020.11.037
36. Warburg O, Wind F, Negelein E, THE METABOLISM OF TUMORS IN THE BODY (1927) J Gen Physiology 8:519–530. https://doi.org/10.1085/jgp.8.6.519
37. Courtnay R, Ngo DC, Malik N, Ververis K, Tortorella SM, Karagiannis TC (2015) Cancer metabolism and the Warburg effect: the role of HIF-1 and PI3K. Mol Biol Rep 42:841–851. https://doi.org/10.1007/s11033-015-3858-x
38. Spilka R, Ernst C, Mehta AK, Haybaeck J (2013) Eukaryotic translation initiation factors in cancer development and progression. Cancer Lett 340:9–21. https://doi.org/10.1016/j.canlet.2013.06.019
39. DeWane G, Salvi AM, DeMali KA (2021) Fueling the cytoskeleton – links between cell metabolism and actin remodeling. J Cell Sci 134:jcs248385. https://doi.org/10.1242/jcs.248385
40. Pawlak G, Helfman DM (2001) Cytoskeletal changes in cell transformation and tumorigenesis. Curr Opin Genet Dev 11:41–47. https://doi.org/10.1016/s0959-437x(00)00154-4
41. Yubero ML, Kosaka PM, Paulo ÁS, Malumbres M, Calleja M, Tamayo J (2020) Effects of energy metabolism on the mechanical properties of Breast cancer cells. Commun Biology 3:590. https://doi.org/10.1038/s42003-020-01330-4
42. Koch S, Claesson-Welsh L (2012) Signal Transduction by Vascular endothelial growth factor receptors. Csh Perspect Med 2:a006502. https://doi.org/10.1101/cshperspect.a006502
43. Hsu M-J, Chen H-K, Lien J-C, Huang Y-H, Huang S-W (2022) Suppressing VEGF-A/VEGFR-2 signaling contributes to the anti-angiogenic effects of PPE8, a Novel Naphthoquinone-based compound, cells. 11:2114. https://doi.org/10.3390/cells11132114

Publisher's Note Springer Nature remains neutral with regard to jurisdictional claims in published maps and institutional affiliations.

Springer Nature or its licensor (e.g. a society or other partner) holds exclusive rights to this article under a publishing agreement with the author(s) or other rightsholder(s); author self-archiving of the accepted manuscript version of this article is solely governed by the terms of such publishing agreement and applicable law.

Authors and Affiliations

Sevinc Yanar[1,2] · Mehmet Sarihan[1] · Murat Kasap[1] · Gurler Akpinar[1] · Kerem Teke[3] · Busra Yaprak Bayrak[4]

✉ Sevinc Yanar
sevincsecer@gmail.com

[1] Faculty of Medicine, Department of Medical Biology, Kocaeli University, Kocaeli, Turkey

[2] Faculty of Medicine, Department of Histology and Embryology, Sakarya University, Korucuk, Sakarya, Turkey

[3] Faculty of Medicine, Department of Urology, Kocaeli University, Kocaeli, Turkey

[4] Faculty of Medicine, Department of Pathology, Kocaeli University, Kocaeli, Turkey